frontiers | Frontiers in Physiology

ORIGINAL RESEARCH
published: 16 June 2022
doi: 10.3389/fphys.2022.916278

Effects of Sarcolemmal Background Ca^{2+} Entry and Sarcoplasmic Ca^{2+} Leak Currents on Electrophysiology and Ca^{2+} Transients in Human Ventricular Cardiomyocytes: A Computational Comparison

Molly E. Streiff[1,2] *and Frank B. Sachse*[1,2]*

[1]Nora Eccles Harrison Cardiovascular Research and Training Institute, University of Utah, Salt Lake City, UT, United States, [2]Department of Biomedical Engineering, University of Utah, Salt Lake City, UT, United States

OPEN ACCESS

Edited by:
Rupamanjari Majumder,
Max Planck Society, Germany

Reviewed by:
Wayne Rodney Giles,
University of Calgary, Canada
Rudi Vennekens,
KU Leuven, Belgium

***Correspondence:**
Frank B. Sachse
frank.sachse@utah.edu

Specialty section:
This article was submitted to Computational Physiology and Medicine, a section of the journal Frontiers in Physiology

Received: 09 April 2022
Accepted: 27 May 2022
Published: 16 June 2022

Citation:
Streiff ME and Sachse FB (2022) Effects of Sarcolemmal Background Ca^{2+} Entry and Sarcoplasmic Ca^{2+} Leak Currents on Electrophysiology and Ca^{2+} Transients in Human Ventricular Cardiomyocytes: A Computational Comparison. Front. Physiol. 13:916278. doi: 10.3389/fphys.2022.916278

The intricate regulation of the compartmental Ca^{2+} concentrations in cardiomyocytes is critical for electrophysiology, excitation-contraction coupling, and other signaling pathways. Research into the complex signaling pathways is motivated by cardiac pathologies including arrhythmia and maladaptive myocyte remodeling, which result from Ca^{2+} dysregulation. Of interest to this investigation are two types of Ca^{2+} currents in cardiomyocytes: 1) background Ca^{2+} entry, i.e., Ca^{2+} transport across the sarcolemma from the extracellular space into the cytosol, and 2) Ca^{2+} leak from the sarcoplasmic reticulum (SR) across the SR membrane into the cytosol. Candidates for the ion channels underlying background Ca^{2+} entry and SR Ca^{2+} leak channels include members of the mechano-modulated transient receptor potential (TRP) family. We used a mathematical model of a human ventricular myocyte to analyze the individual contributions of background Ca^{2+} entry and SR Ca^{2+} leak to the modulation of Ca^{2+} transients and SR Ca^{2+} load at rest and during action potentials. Background Ca^{2+} entry exhibited a positive relationship with both $[Ca^{2+}]_i$ and $[Ca^{2+}]_{SR}$. Modulating SR Ca^{2+} leak had opposite effects of background Ca^{2+} entry. Effects of SR Ca^{2+} leak on Ca^{2+} were particularly pronounced at lower pacing frequency. In contrast to the pronounced effects of background and leak Ca^{2+} currents on Ca^{2+} concentrations, the effects on cellular electrophysiology were marginal. Our studies provide quantitative insights into the differential modulation of compartmental Ca^{2+} concentrations by the background and leak Ca^{2+} currents. Furthermore, our studies support the hypothesis that TRP channels play a role in strain-modulation of cardiac contractility. In summary, our investigations shed light on the physiological effects of the background and leak Ca^{2+} currents and their contribution to the development of disease caused by Ca^{2+} dysregulation.

Keywords: calcium, cardiomyocyte, sarcolemma, sarcoplasmic reticulum, leak

INTRODUCTION

Ca^{2+} concentrations are dynamically controlled in cardiomyocytes by a complex regulatory system comprising ion channels, transporters, exchangers, regulatory proteins, and ion buffers. Intricately regulated levels of Ca^{2+} concentrations are critical for electrical activity, excitation-contraction coupling, and other signaling pathways. In many cardiac diseases, the delicate balance of Ca^{2+} cycling is perturbed. Ca^{2+} dysregulation underlies maladaptive cardiac remodeling. A complete understanding of all components of Ca^{2+} handling is essential for the development of therapeutic strategies to attenuate cardiac pathologies.

Many ion channels underlying the Ca^{2+} signaling in cardiomyocytes are well characterized. Ca^{2+} signaling related to excitation-contraction coupling primarily relies on sarcolemmal Ca^{2+} entry through voltage-gated L-type Ca^{2+} channels (LTCC) to trigger Ca^{2+}-induced Ca^{2+} release from the sarcoplasmic reticulum (SR) through ryanodine receptors (RyR), and, subsequently, Ca^{2+} extrusion *via* the sodium-calcium exchanger (NCX) and reuptake into the SR through sarco/endoplasmic Ca^{2+}-ATPase (SERCA). Other Ca^{2+} currents contribute to the modulation of Ca^{2+} concentrations in cardiomyocytes as well. Of interest to this study are background Ca^{2+} entry through the sarcolemma and SR Ca^{2+} leak. Understanding of the physiological role of these Ca^{2+} currents is still incomplete.

Beyond Ca^{2+} transport across the sarcolemma from the extracellular space into the cytosol through LTCC and NCX, sarcolemmal Ca^{2+} transport comprises background Ca^{2+} entry. In resting cardiomyocytes, $[Ca^{2+}]_i$ is of the order of 100 nM, which indicates the existence of a background Ca^{2+} entry pathway to balance the Ca^{2+} efflux of NCX (Eisner et al., 2020). Resting ventricular myocytes depleted of Ca^{2+} stores with caffeine are able to reload the SR by a mechanism that involves extracellular Ca^{2+}, demonstrating further evidence of background Ca^{2+} entry (Terracciano and Macleod, 1996). Based on studies measuring background Ca^{2+} influx in rat ventricular myocytes of the order of 2–5 μmol/L per second (Choi et al., 2000) or 4 μmol/L per second (Sankaranarayanan et al., 2017), the background Ca^{2+} entry is approximately 10% of the influx through LTCC current (5–10 μmol/L each action potential) at normal heart rates (Eisner et al., 2020). The identity of background Ca^{2+} flux is still poorly defined, but several channels have been suggested as contributors.

One study identified a Ca^{2+} entry mechanism that is blocked by the nonspecific agent gadolinium (Gd^{3+}) (Kupittayanant et al., 2006). Connexin hemichannels are candidates for background Ca^{2+} entry since they can be inhibited by Gd^{3+} (Stout et al., 2002). While connexin hemichannels primarily form pairs to allow ion fluxes between cells at intercalated discs, some are present as hemichannels in the surface membrane of a single cell (Wang et al., 2012; Leybaert et al., 2017) and may, therefore, provide a route for Ca^{2+} entry. However, primary candidates for background Ca^{2+} entry include members of the family of Transient Receptor Potential (TRP) channels, which are also sensitive to Gd^{3+}. The *mdx* mouse model of muscular dystrophy exhibits $[Ca^{2+}]_i$ and $[Na^+]_i$ overload that can be blocked by Gd^{3+}, and the increase in cation entry has been suggested to involve TRPC channels (Mijares et al., 2014). Myocytes from old *mdx* mice exhibit increased expression of a putative stretch-activated channel (SAC), TRPC1. Elevated $[Ca^{2+}]_i$ levels can also be reduced to $[Ca^{2+}]_i$ levels of WT myocytes when exposed to SAC blockers streptomycin or GsMTx-4 (Williams and Allen, 2007; Ward et al., 2008). Upregulated TRPC1 also contributes to increased $[Ca^{2+}]_i$ through SAC in hypertrophic myocardium of rats following isoproterenol injection (Chen et al., 2013). Background Ca^{2+} entry involved in maladaptive cardiac remodeling was more recently shown to critically depend on both TRPC1 and TRPC4 (Camacho Londono et al., 2015, Camacho Londoño et al., 2021). TRPC6 channels have also been shown to modulate cytosolic Ca^{2+} transients and SR Ca^{2+} load through sarcolemmal Ca^{2+} entry (Ahmad et al., 2020). Furthermore, TRPV4 can modulate Ca^{2+} transients and SR load, and participates in hypoosmotic stress-induced cardiomyocyte Ca^{2+} entry (Rubinstein et al., 2014; Jones et al., 2019).

Ca^{2+} transport across the SR membrane from the intracellular store into the cytosol is known as SR Ca^{2+} leak. During an action potential, activation of RyR clusters triggered by Ca^{2+} entry through LTCC results in a synchronized release of a large amount of Ca^{2+} from the SR that forms the Ca^{2+} transient and leads to cardiomyocyte contraction. Activation of RyR clusters causes Ca^{2+} sparks. These sparks are an important pathway for SR Ca^{2+} leak. RyR Ca^{2+} leak can occur also through a mechanism independent of sparks (Santiago et al., 2010). Further, total SR Ca^{2+} leak includes a component separate from RyRs (Zima et al., 2010). Many candidates have been suggested as components of this leak, yet it is still ill-defined. A candidate is the inositol 1,4,5-trisphosphate (IP_3) receptor (IP_3R), which is a Ca^{2+} release channel expressed at lower densities than RyRs in cardiomyocytes and found upregulated in heart failure (HF) (Go et al., 1995; Ai et al., 2005) and therefore may be a relevant contributor to SR Ca^{2+} leak (Zima et al., 2010). Members of the TRP family have also been suggested to contribute to SR Ca^{2+} leak. TRPC1 was found to operate as a SR Ca^{2+} leak channel in skeletal muscle (Berbey et al., 2009) and more recently in cardiomyocytes (Hu et al., 2020). Additional evidence suggests contribution of TRPC6, TRPM8, TRPP2, and TRPV1 to endoplasmic reticulum Ca^{2+} leak in various cell types, although characterization is still incomplete for cardiomyocytes (Lemos et al., 2021).

TRP channels constitute primary candidates for explaining background and leak Ca^{2+} currents through both the sarcolemma and the SR membrane. Interestingly, many members of the TRP family are known to be modulated by stretch (Inoue et al., 2009; Reed et al., 2014; Peyronnet et al., 2016). Cardiomyocyte contractility is known to respond to mechanical stretch in two phases: a rapid and a slow response (Calaghan and White, 1999). The rapid response is the cellular basis for the Frank-Starling Mechanism (FSM). It relies primarily on myofilament overlap and alteration of myofilament Ca^{2+} sensitivity, and does not involve changes in Ca^{2+} transients. The slow response has been termed slow force response (SFR) or stress-induced slow increase

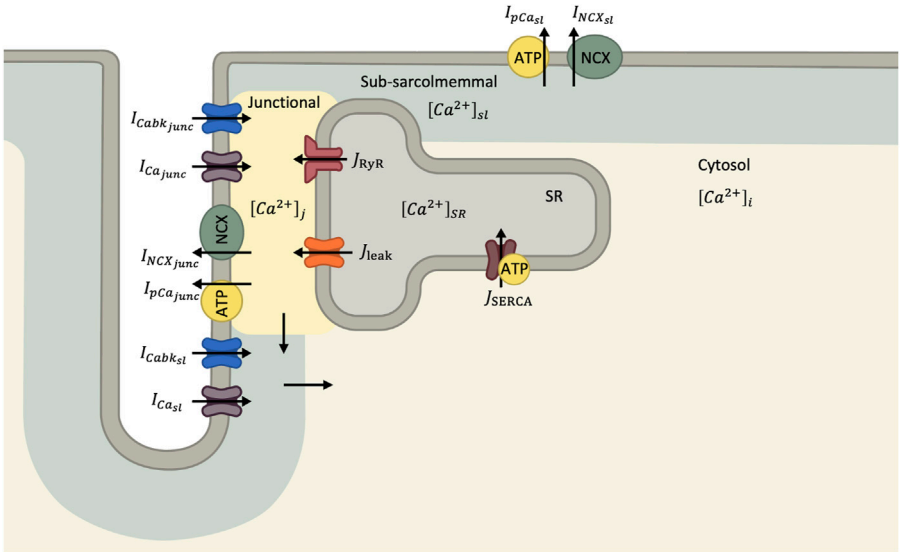

FIGURE 1 | Diagram of Ca^{2+} handling components in human ventricular myocyte model (Grandi et al., 2010). In this mathematical model, the cytosol is divided into junction, sub-sarcolemmal and bulk compartments. Ca^{2+} currents through the sarcolemma enter both the junctional and sub-sarcolemmal compartments before diffusing to the bulk cytosol.

in contractility (SSC), describing the gradual increase in twitch force corresponding to an increase in $[Ca^{2+}]_i$ transients that develops over several minutes when stretch is sustained. Members of the TRP family are likely candidates for mechanotransduction of the SFR.

Though background and leak Ca^{2+} currents are still poorly defined, they may play important roles in regulating Ca^{2+} homeostasis and contractility and altered Ca^{2+} dynamics in cardiac disease. The lack of complete understanding of the identity and mechanics of these channels, in addition to their relatively small amplitude compared to the voltage-gated Ca^{2+} channels, make them difficult to study *in vivo*. A computational model provides the advantage to study the currents and their roles in isolation from other cellular mechanisms. In this study, we use a mathematical model of a human ventricular myocyte to analyze the individual contributions of background Ca^{2+} entry and SR Ca^{2+} leak to the modulation of Ca^{2+} transients and SR Ca^{2+} load. We also assess the effects of the Ca^{2+} currents on cellular electrophysiology.

MATERIALS AND METHODS

Mathematical Model of Ventricular Myocyte

We applied a mathematical model of a human ventricular myocyte (Grandi et al., 2010). The model and subsequent analyses were executed in MATLAB (R2020b). The model includes subsarcolemmal and junctional compartments beyond the cytosol compartment. Total background Ca^{2+} current (I_{Cabk}) through the sarcolemma is defined as a summation of junctional ($I_{Cabk,\ junc}$) and subsarcolemmal ($I_{Cabk,sl}$) components:

$$I_{Cabk_{junc}} = F_{junc} G_{bkg} \left(V_m - E_{Ca_{junc}}\right), \quad (1)$$

$$I_{Cabk_{sl}} = F_{sl} G_{bkg} \left(V_m - E_{Ca_{sl}}\right), \quad (2)$$

$$I_{Cabk} = I_{Cabk_{junc}} + I_{Cabk_{sl}}, \quad (3)$$

where $F_{junc} = 0.11$ and $F_{sl} = 0.89$ are constants that determine the fraction of total background current corresponding to the junctional and subsarcolemmal spaces, respectively, G_{bkg} is the maximum conductance (5.513e-4 A/F) of the channels, V_m is the transmembrane voltage, and $E_{Ca,junc}$ and $E_{Ca,sl}$ are Nernst potentials corresponding to the junctional and subsarcolemmal spaces, respectively. SR Ca^{2+} leak (J_{leak}) describes the Ca^{2+} flux out of the SR:

$$J_{leak} = K_{leak} \left([Ca^{2+}]_{SR} - [Ca^{2+}]_j \right), \quad (4)$$

where K_{leak} is the leak constant (5.348e-6/ms), and $[Ca^{2+}]_{SR}$ and $[Ca^{2+}]_j$ describe the Ca^{2+} concentrations in the SR and junctional space, respectively. In this study, we modulated G_{bkg} and K_{leak} independently and in conjunction to investigate the effects of altered sarcolemmal Ca^{2+} entry and altered SR Ca^{2+} leak, respectively.

A graphical summary of the Ca^{2+} currents in the cell model is shown in **Figure 1**. The total Ca^{2+} current into the junctional ($I_{Ca,tot,junc}$) and subsarcolemmal ($I_{Ca,tot,sl}$) compartments are determined by **Eqs 5**, **6**, respectively:

$$I_{Ca_{tot\ junc}} = I_{Ca_{junc}} + I_{Cabk_{junc}} + I_{pCa_{junc}} - 2 \cdot I_{NCX_{junc}}, \quad (5)$$

$$I_{Ca_{tot\ sl}} = I_{Ca_{sl}} + I_{Cabk_{sl}} + I_{pCa_{sl}} - 2 \cdot I_{NCX_{sl}}, \quad (6)$$

where I_{Ca} describes the L-type Ca^{2+} current, I_{pCa} describes the sarcolemmal Ca^{2+} pump current, and I_{NCX} describes the NCX current.

The rate of change of Ca^{2+} concentrations in the junctional compartment $[Ca^{2+}]_j$, subsarcolemmal compartment $[Ca^{2+}]_{sl}$, bulk cytosol $[Ca^{2+}]_i$, and SR $[Ca^{2+}]_{SR}$ are given by:

$$\frac{d[Ca^{2+}]_j}{dt} = -I_{Ca_{tot_{junc}}} \cdot \frac{C_{mem}}{V_{junc} \cdot 2 \cdot F} + \frac{J_{Ca_{juncsl}}}{V_{junc}} \cdot \left([Ca^{2+}]_{sl} - [Ca^{2+}]_j\right) - J_{CaB_{junction}} + J_{RYR} \cdot \frac{V_{sr}}{V_{junc}} + J_{leak} \cdot \frac{V_{myo}}{V_{junc}}, \quad (7)$$

$$\frac{d[Ca^{2+}]_{sl}}{dt} = -I_{Ca_{tot_{sl}}} \cdot \frac{C_{mem}}{V_{sl} \cdot 2 \cdot F} + \frac{J_{Ca_{juncsl}}}{V_{sl}} \cdot \left([Ca^{2+}]_j - [Ca^{2+}]_{sl}\right) + \frac{J_{Ca_{slmyo}}}{V_{sl}} \cdot \left([Ca^{2+}]_i - [Ca^{2+}]_{sl}\right) - J_{CaB_{sl}}, \quad (8)$$

$$\frac{d[Ca^{2+}]_i}{dt} = -J_{SERCA} \cdot \frac{V_{sr}}{V_{myo}} - J_{CaB_{cytosol}} + \frac{J_{Ca_{slmyo}}}{V_{myo}} \cdot \left([Ca^{2+}]_{sl} - [Ca^{2+}]_i\right), \quad (9)$$

$$\frac{d[Ca^{2+}]_{SR}}{dt} = J_{SERCA} - \left(J_{leak} \cdot \frac{V_{myo}}{V_{sr}} + J_{RyR}\right) - \frac{dCsqn_b}{dt}, \quad (10)$$

where C_{mem} is the membrane capacitance, F is Faraday's constant, V_{junc} is the volume of the junctional compartment, V_{sl} is the volume of the subsarcolemmal compartment, V_{myo} is the volume of the bulk cytosol, and V_{sr} is the volume of the SR. $J_{Ca,juncsl}$ is the rate of Ca^{2+} flux from junctional to subsarcolemmal compartments and $J_{Ca,slmyo}$ is the rate of Ca^{2+} flux from the subsarcolemmal compartment to bulk cytosol. J_{RYR} describes the SR Ca^{2+} release and J_{SERCA} describes the SR Ca^{2+} pump. Ca^{2+} buffering is described by $J_{Ca,B,junction}$ in the junctional compartment, $J_{Ca,B,sl}$ in the subsarcolemmal compartment, $J_{Ca,B,cytosol}$ in the bulk cytosol, and $dCsqn_b/dt$ in the SR. We refer to (Grandi et al., 2010) for more details and the equations describing the mathematical model.

Evaluating the Effects of Background and Leak Ca^{2+} Currents on Ca^{2+} Concentrations

To investigate the effects of altered background Ca^{2+} entry, we modulated G_{bkg} from 0 to 300% of its default value, 5.513e-4 A/F. To investigate the effects of altered SR Ca^{2+} leak, we modulated K_{leak} from 0 to 300% of its default value, 5.348e-6 ms^{-1}. Simulation durations were 1 min to establish steady state. We analyzed the last beat. We performed sensitivity analyses for the modulation of G_{bkg} and K_{leak} independently on measurements of resting V_m, maximum V_m, action potential duration to 90% repolarization (APD_{90}), diastolic $[Ca^{2+}]_i$, systolic $[Ca^{2+}]_i$, $[Ca^{2+}]_i$ amplitude, diastolic $[Ca^{2+}]_{SR}$, systolic $[Ca^{2+}]_{SR}$, and $[Ca^{2+}]_{SR}$ amplitude. Sensitivity analyses of each measured parameter were then normalized to the measurement of the default model values and fit to the quadratic equation:

$$y(x) = Ax^2 + Bx + C, \quad (11)$$

where x is the fraction (%) of default G_{bkg} or K_{leak}. We evaluated the factor of the quadratic term, A, the linear term, B, and the constant term, C, of this fit for relative comparisons of the effects of modulated background Ca^{2+} current or modulated SR Ca^{2+} leak. This analysis was repeated for the model ran at 1, 2, and 3 Hz electrical excitation.

We subsequently performed a dual-sensitivity analysis for the modulations of G_{bkg} and K_{leak} to understand how the two Ca^{2+} currents interact and influence Ca^{2+} handling in the cardiomyocyte together.

RESULTS

Qualitative Changes in V_m, $[Ca^{2+}]_i$, and $[Ca^{2+}]_{SR}$ When Background Ca^{2+} Entry is Modulated

We first examined the changes in V_m, $[Ca^{2+}]_i$, and $[Ca^{2+}]_{SR}$ following modulation of the background Ca^{2+} entry current, I_{Cabk}, at pacing rates of 1, 2 and 3 Hz (**Figure 2**). Changes to features of the action potential were minimal (**Figure 2A**). Resting V_m exhibited a positive relationship with % G_{bkg} (**Figure 2B**), while maximum depolarization exhibited a negative relationship (**Figure 2C**) with increasing background Ca^{2+} current. APD_{90} showed a positive relationship, where increased background Ca^{2+} entry lengthens the time for repolarization (**Figure 2D**). We measured diastolic and systolic values, as well as amplitude of $[Ca^{2+}]_i$ transients (**Figure 2E**). All measurements demonstrate positive relationships with increasing background Ca^{2+} entry; the increase in systolic $[Ca^{2+}]_i$ (**Figure 2F**) is greater than the increase in diastolic $[Ca^{2+}]_i$ (**Figure 2G**), especially at the slowest pacing rate, so the amplitude increases a considerable amount (**Figure 2H**). We measured the same parameters of $[Ca^{2+}]_{SR}$ transients, which also demonstrate an increase in amplitude caused by increased background Ca^{2+} entry (**Figures 2I,L**). The release was initiated from increased diastolic $[Ca^{2+}]_{SR}$ (**Figure 2J**) and ended in reduced systolic $[Ca^{2+}]_{SR}$ (**Figure 2K**). The relationships between background Ca^{2+} entry and features of the $[Ca^{2+}]_{SR}$ transient were also augmented at the slowest pacing rate.

Qualitative Changes in V_m, $[Ca^{2+}]_i$, and $[Ca^{2+}]_{SR}$ When SR Ca^{2+} Leak is Modulated

Changes following independent modulation of the SR Ca^{2+} leak current, J_{leak}, were also examined (**Figure 3**). The effects of modulating K_{leak} on V_m were small (**Figure 3A**). Resting V_m exhibited a slight positive relationship (**Figure 3B**). Maximum V_m increased with increasing K_{leak} at 1 Hz pacing but decreased with K_{leak} at 2 and 3 Hz pacing (**Figure 3C**). Repolarization time measured as APD_{90} was unaltered by modulations of K_{leak} (**Figure 3D**). Diastolic $[Ca^{2+}]_i$ was also relatively unaffected by modulations of K_{leak} (**Figures 3E,F**). However systolic $[Ca^{2+}]_i$ and thus also $[Ca^{2+}]_i$ amplitude decreased with increasing K_{leak} (**Figures 3G,H**). The effect was strongest at the slowest pacing frequency of 1 Hz. Alterations in $[Ca^{2+}]_{SR}$ were also strongest at 1 Hz pacing. Diastolic $[Ca^{2+}]_{SR}$ exhibited a negative relationship with K_{leak} (**Figure 3J**), while systolic $[Ca^{2+}]_{SR}$ exhibits a positive

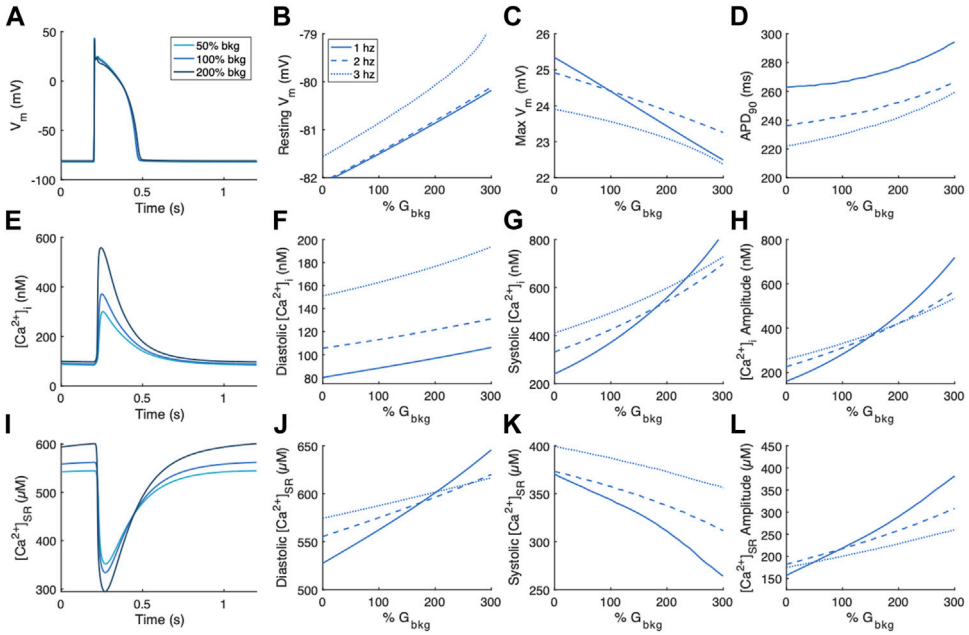

FIGURE 2 | Effects of modulating the background Ca^{2+} entry current, $I_{Cabk,}$ on V_m, $[Ca^{2+}]_i$, and $[Ca^{2+}]_{SR.}$ **(A)** Example action potentials for 50% and 200% G_{bkg} at 1 Hz pacing. Sensitivity analyses of modulating G_{bkg} on measurements of **(B)** resting V_m, **(C)** maximum V_m, and **(D)** time to 90% repolarization at 1, 2 and 3 Hz pacing. **(E)** Example $[Ca^{2+}]_i$ transients for 50% and 200% G_{bkg} at 1 Hz pacing. Sensitivity analyses of modulating G_{bkg} on measurements of **(F)** diastolic $[Ca^{2+}]_i$, **(G)** systolic $[Ca^{2+}]_i$, and **(H)** $[Ca^{2+}]_i$ amplitude at 1, 2 and 3 Hz pacing. **(I)** Example $[Ca^{2+}]_{SR}$ transients for 50% and 200% G_{bkg} at 1 Hz pacing. Sensitivity analyses of modulating G_{bkg} on measurements of **(J)** diastolic $[Ca^{2+}]_{SR}$, **(K)** systolic $[Ca^{2+}]_{SR}$, and **(L)** $[Ca^{2+}]_{SR}$ amplitude at 1, 2 and 3 Hz pacing.

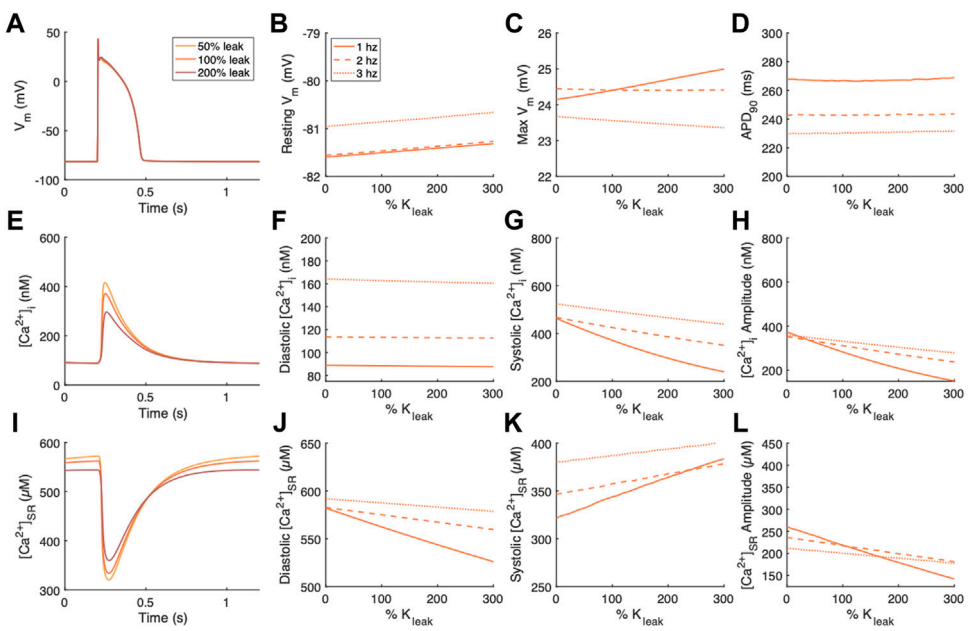

FIGURE 3 | Effects of modulating the SR Ca^{2+} leak flux, $J_{leak,}$ on V_m, $[Ca^{2+}]_i$, and $[Ca^{2+}]_{SR.}$ **(A)** Example action potentials for 50% and 200% K_{leak} at 1 Hz pacing. Sensitivity analyses of modulating K_{leak} on measurements of **(B)** resting V_m, **(C)** maximum V_m, and **(D)** time to 90% repolarization at 1, 2 and 3 Hz pacing. **(E)** Example $[Ca^{2+}]_i$ transients for 50% and 200% K_{leak} at 1 Hz pacing. Sensitivity analyses of modulating K_{leak} on measurements of **(F)** diastolic $[Ca^{2+}]_i$, **(G)** systolic $[Ca^{2+}]_i$, and **(H)** $[Ca^{2+}]_i$ amplitude at 1, 2 and 3 Hz pacing. **(I)** Example $[Ca^{2+}]_{SR}$ transients for 50% and 200% K_{leak} at 1 Hz pacing. Sensitivity analyses of modulating K_{leak} on measurements of **(J)** diastolic $[Ca^{2+}]_{SR}$, **(K)** systolic $[Ca^{2+}]_{SR}$, and **(L)** $[Ca^{2+}]_{SR}$ amplitude at 1, 2 and 3 Hz pacing.

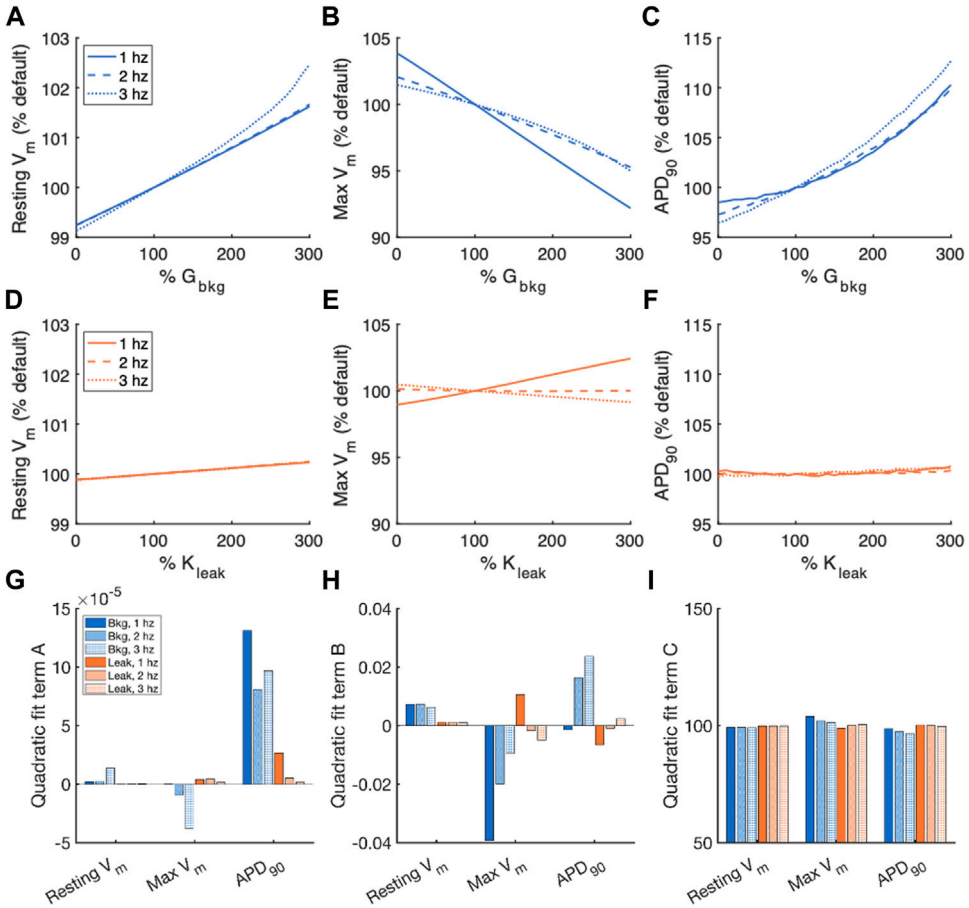

FIGURE 4 | Summary of effects of modulating G_{bkg} or K_{leak} independently on V_m. Sensitivity analyses of modulating G_{bkg} on measurements of **(A)** resting V_m, **(B)** maximum V_m, and **(C)** time to 90% repolarization normalized by the default model parameters. Sensitivity analyses of modulating K_{leak} on measurements of **(D)** resting V_m, **(E)** maximum V_m, and **(F)** time to 90% repolarization normalized by the default model parameters. Summary of the **(G)** quadratic term, **(H)** linear term and **(I)** constant term calculated by quadratic polynomial fits to the normalized sensitivity analyses in **(A–H)**.

relationship with K_{leak} (**Figure 3K**), both contributing to reduced $[Ca^{2+}]_{SR}$ amplitude with increased K_{leak} (**Figure 3L**).

Summary and Comparison of Independent Modulation of Background and Leak Currents

For comparison of the effects of altered G_{bkg} or K_{leak} on features of the action potential, we normalized the measurements of resting V_m, maximum V_m, and APD_{90} to the default measurements from the model for the given pacing frequency (**Figures 4A–F**). The relationships of measured vs. modified parameter, both represented as fraction (%) vs. default values, were fit to a 2nd order polynomial model for quantification of the effects (**Figures 4G–I**). The quadratic term of the fit is negligible for resting V_m and maximum V_m, demonstrating that these measurements exhibit primarily linear relationships with G_{bkg} and K_{leak} (**Figure 4G**). However, the polynomial fit of APD_{90} to G_{bkg} has a strong quadratic term, demonstrating a non-linear relationship between APD_{90} and G_{bkg} (**Figure 4G**). Since the relationships of resting V_m and maximum V_m are primarily linear, the linear term of the quadratic polynomial fit demonstrates the sensitivity of the measurements to changes in G_{bkg} or K_{leak} (**Figure 4H**). Both G_{bkg} and K_{leak} modulation have a positive relationship with resting V_m, but the changes are negligible for K_{leak} and minimal for G_{bkg}, never exceeding an increase greater than 2% of the default model's resting V_m. Maximum V_m had a strong negative linear relationship with G_{bkg} for all pacing frequencies, especially at 1 Hz pacing. Maximum V_m had a positive linear relationship with K_{leak} at 1 Hz pacing but negatives linear relationship for 2 and 3 Hz. The constant of the quadratic polynomial model represents the measurements for the modulated currents set to 0 (**Figure 4I**). These results revealed that resting V_m was largely unchanged by pacing rate. Maximum V_m was slightly increased with no I_{Cabk} and slightly reduced with no J_{leak} at 1 Hz and slightly increased with no J_{leak} at 3 Hz. APD_{90} decreased without I_{Cabk} but remained unchanged without K_{leak}.

Figure 5 contains a summary of $[Ca^{2+}]_i$ normalized by measurements of the default model for the sensitivity

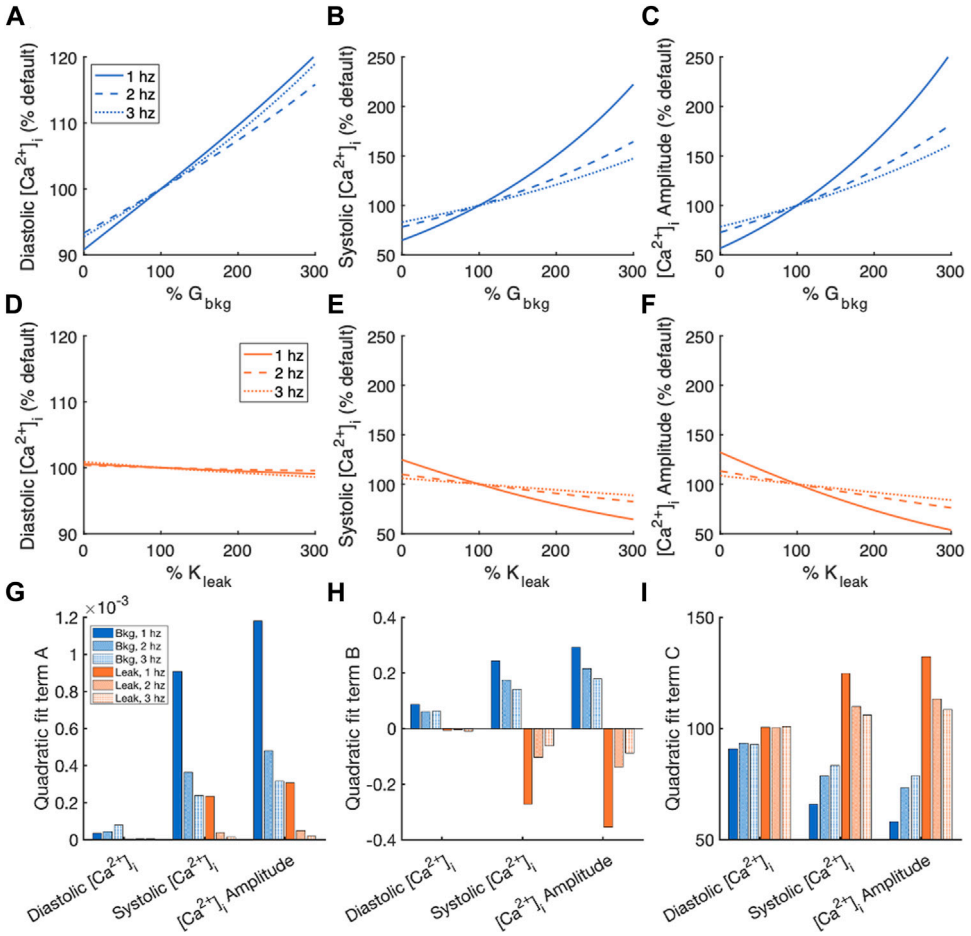

FIGURE 5 | Summary of effects of modulating G_{bkg} or K_{leak} independently on $[Ca^{2+}]_i$. Sensitivity analyses of modulating G_{bkg} on measurements of **(A)** diastolic $[Ca^{2+}]_i$, **(B)** systolic $[Ca^{2+}]_i$, and **(C)** $[Ca^{2+}]_i$ amplitude normalized by the default model parameters. Sensitivity analyses of modulating K_{leak} on measurements of **(D)** diastolic $[Ca^{2+}]_i$, **(E)** systolic $[Ca^{2+}]_i$, and **(F)** $[Ca^{2+}]_i$ amplitude normalized by the default model parameters. Summary of the **(G)** quadratic term, **(H)** linear term and **(I)** constant term calculated by quadratic polynomial fits to the normalized sensitivity analyses in **(A–H)**.

analyses of G_{bkg} and K_{leak} modulation. The relationships of measured parameter vs. modified parameter, both represented as % default values, were fit to a 2nd order polynomial model for quantification of the effects. The quadratic term indicates nonlinearity of the relationship (**Figure 5G**). The quadratic term of the diastolic $[Ca^{2+}]_i$ fits were marginal, indicating a primarily linear relationship. For both G_{bkg} and K_{leak} modulations, we noticed a nonlinearity associated with systolic $[Ca^{2+}]_i$ and consequently the $[Ca^{2+}]_i$ amplitude, with the greatest degree of nonlinearity associated with the lowest pacing frequency. The linear term of the quadratic fit showed a strong linear sensitivity of the measured parameter to changes in G_{bkg} or K_{leak} (**Figure 5H**). The positive sign of this term for G_{bkg} modulations for each measurement, diastolic, systolic, and amplitude, demonstrates the positive relationship of these parameters with G_{bkg}, with greater slope of the relationship for systolic and amplitude measurements. The linear term for diastolic $[Ca^{2+}]_i$ sensitivity to K_{leak} was negative but very small, demonstrating that diastolic $[Ca^{2+}]_i$ exhibits negligible sensitivity to SR Ca^{2+} leak. The relationship of systolic $[Ca^{2+}]_i$ sensitivity to K_{leak} was negative, with the largest value for 1 Hz pacing. The same is true for $[Ca^{2+}]_i$ transient amplitude. The constant term of the quadratic polynomial fits corresponds to the % default if the modulated channel were 0 (**Figure 5I**). Elimination of I_{Cabk} resulted in a reduction of diastolic $[Ca^{2+}]_i$, systolic $[Ca^{2+}]_i$, and $[Ca^{2+}]_i$ amplitude, with the greatest reductions at 1 Hz pacing. Elimination of J_{leak} did not affect diastolic $[Ca^{2+}]_i$, but results in increased systolic $[Ca^{2+}]_i$ and $[Ca^{2+}]_i$ amplitude, especially at 1 Hz pacing.

Measurements of diastolic and systolic $[Ca^{2+}]_{SR}$ and $[Ca^{2+}]_{SR}$ transient amplitude, normalized by measurements of the default model, for the sensitivity analyses of G_{bkg} and K_{leak} modulations are summarized in **Figure 6**. Again, a 2nd order polynomial model for the normalized sensitivity analyses provided information about the relationships. The quadratic term of the fits demonstrates that systolic $[Ca^{2+}]_{SR}$ and $[Ca^{2+}]_{SR}$ transient amplitude both exhibited nonlinearity in the relationship to

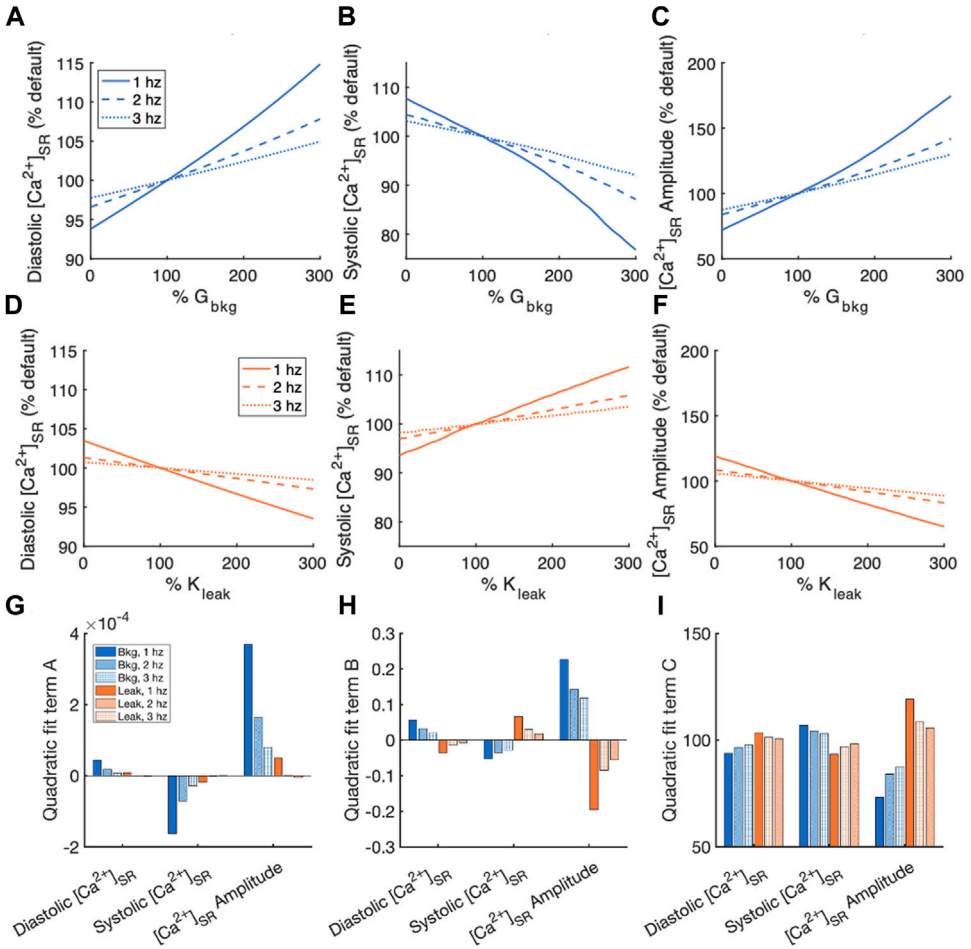

FIGURE 6 | Summary of effects of modulating G_{bkg} or K_{leak} independently on $[Ca^{2+}]_{SR}$. Sensitivity analyses of modulating G_{bkg} on measurements of **(A)** diastolic $[Ca^{2+}]_{SR}$, **(B)** systolic $[Ca^{2+}]_{SR}$, and **(C)** $[Ca^{2+}]_{SR}$ amplitude normalized by the default model parameters. Sensitivity analyses of modulating K_{leak} on measurements of **(D)** diastolic $[Ca^{2+}]_{SR}$, **(E)** systolic $[Ca^{2+}]_{SR}$, and **(F)** $[Ca^{2+}]_{SR}$ amplitude normalized by the default model parameters. Summary of the **(G)** quadratic term, **(H)** linear term and **(I)** constant term calculated by quadratic polynomial fits the normalized sensitivity analyses in **(A–H)**.

modulated G_{bkg} (**Figure 6G**). The linear term of the relationships demonstrated the best representation sensitivity of the measurements to G_{bkg} or K_{leak} modulation (**Figure 6H**). The sign of this term was opposite for each measured parameter for G_{bkg} vs. K_{leak} modulation but similar in amplitude. While the changes to $[Ca^{2+}]_{SR}$ transients all contributed to a positive correlation between G_{bkg} and $[Ca^{2+}]_{SR}$ transient amplitude, the opposite changes all contribute to a negative correlation between K_{leak} and $[Ca^{2+}]_{SR}$ transient amplitude. The constant term of the polynomial model, which corresponds to the % of default model measurements if the current is set to 0, showed that in the absence of I_{Cabk}, diastolic $[Ca^{2+}]_{SR}$ is lower, systolic $[Ca^{2+}]_{SR}$ is higher, and $[Ca^{2+}]_{SR}$ amplitude is reduced (**Figure 6I**). In the absence of J_{leak}, diastolic $[Ca^{2+}]_{SR}$ was slightly elevated, systolic $[Ca^{2+}]_{SR}$ was reduced, and the amplitude of $[Ca^{2+}]_{SR}$ was greater. The effects on all measurements of $[Ca^{2+}]_{SR}$ following modulation of G_{bkg} or K_{leak} were stronger at 1 Hz pacing than at faster pacing frequencies.

Effects of Dual Modulation of Background Ca^{2+} Entry and SR Ca^{2+} Leak on Vm, $[Ca^{2+}]_i$, and $[Ca^{2+}]_{SR}$

With a thorough understanding of how G_{bkg} and K_{leak} modulations independently affect features of the action potential, $[Ca^{2+}]_i$ and $[Ca^{2+}]_{SR}$ transients, we subsequently performed a dual-parameter sensitivity analysis of G_{bkg} and K_{leak} together for 1 Hz pacing (**Figure 7**). Resting V_m is affected minimally by G_{bkg}, and negligibly by K_{leak}, apparent by the nearly horizontal contour lines (**Figure 7A**). Both increasing G_{bkg} and increasing K_{leak} resulted in increased V_m, but increasing G_{bkg} makes a larger contribution. Maximum V_m was modulated in opposite directions by G_{bkg} and K_{leak} (**Figure 7B**). Increasing G_{bkg} reduces maximum V_m while increasing K_{leak} increased maximum V_m, but G_{bkg} is the slightly more dominant effect. APD_{90} experienced the greatest increase at large increases in G_{bkg} and small K_{leak} (**Figure 7C**).

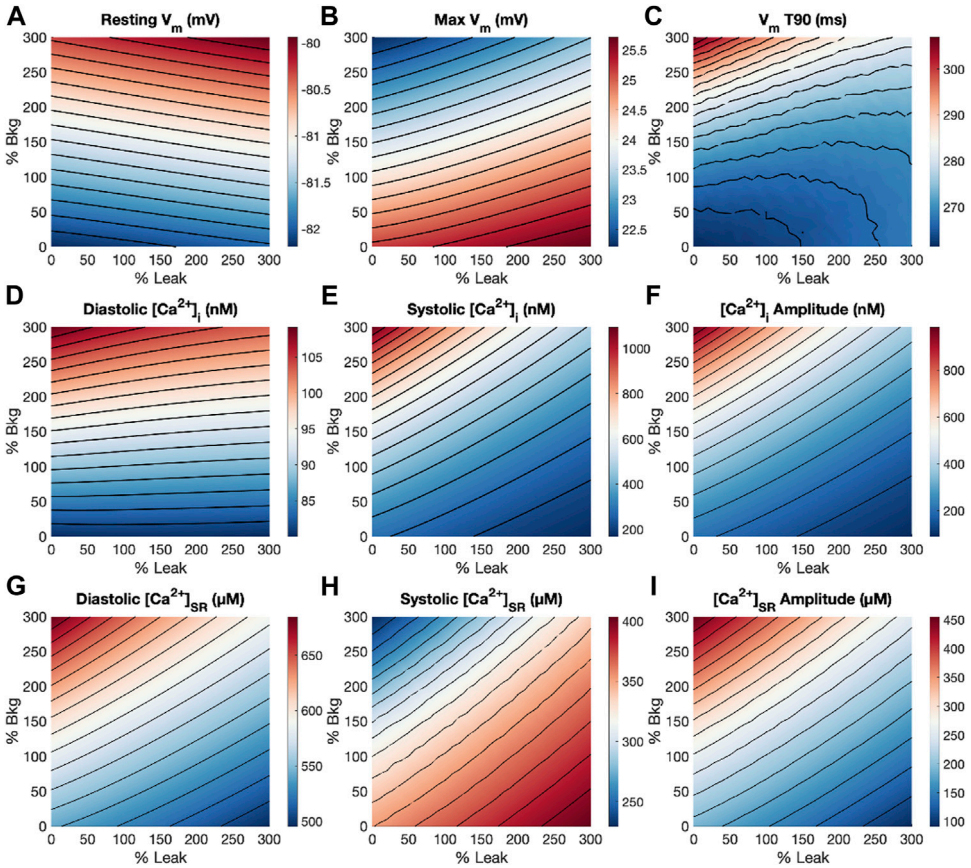

FIGURE 7 | Dual-parameter sensitivity analysis of modulating G_{bkg} and K_{leak} at 1 Hz pacing. Surface plots with contour lines for measurements of **(A)** resting V_m, **(B)** maximum V_m, **(C)** APD_{90}, **(D)** diastolic $[Ca^{2+}]_i$, **(E)** systolic $[Ca^{2+}]_i$, **(F)** $[Ca^{2+}]_i$ amplitude, **(G)** diastolic $[Ca^{2+}]_{SR}$, **(H)** systolic $[Ca^{2+}]_{SR}$, and **(I)** $[Ca^{2+}]_{SR}$ amplitude.

Diastolic $[Ca^{2+}]_i$ was primarily affected by a positive relationship to G_{bkg}, while K_{leak} appeared to make no contribution (**Figure 7D**). Interestingly, for all other $[Ca^{2+}]_i$ and $[Ca^{2+}]_{SR}$ measurements, the opposing effects of G_{bkg} and K_{leak} appeared to balance with a very similar linear relationship (**Figures 7E–I**). The contour lines of the dual-parameter sensitivity analyses for systolic $[Ca^{2+}]_i$, $[Ca^{2+}]_i$ amplitude, diastolic and systolic $[Ca^{2+}]_{SR}$ and $[Ca^{2+}]_{SR}$ amplitude all exhibited strikingly similar slopes.

If both background and leak currents were modulated along this relationship, measured parameters remained relatively unchanged and only diastolic $[Ca^{2+}]_i$ increased. An example of balanced background Ca^{2+} entry and SR Ca^{2+} leak demonstrates that a G_{bkg} value 200% of default and K_{leak} value of 270% default provided a balanced effect and canceled out the opposing modulations on systolic $[Ca^{2+}]_i$ and diastolic $[Ca^{2+}]_{SR}$ load, while diastolic $[Ca^{2+}]_i$ was elevated 7.9% (**Figure 8**).

DISCUSSION

In this study, we evaluated the contributions of background Ca^{2+} entry and SR Ca^{2+} leak to V_m and Ca^{2+} concentrations in the SR and cytosol in cardiomyocytes *in silico*. Our investigations shed light on the differential effects of background and leak Ca^{2+} currents in physiology, and also provide insight into their contributions to disease development due to Ca^{2+} dysfunction. Below, we discussed background Ca^{2+} entry as a mechanism to positively modulate Ca^{2+} entry and SR Ca^{2+} leak as a critical balancing mechanism to maintain homeostasis.

Background Ca^{2+} Entry Positively Modulates Ca^{2+} Concentrations

Our results show that background Ca^{2+} entry has a positive relationship with diastolic $[Ca^{2+}]_i$ and $[Ca^{2+}]_{SR}$, and the amplitude of their transients (**Figure 2**). The small increase in diastolic $[Ca^{2+}]_i$ is the direct result of an increase in background Ca^{2+} entry, and the increase in $[Ca^{2+}]_{SR}$ follows as SERCA responds to pump the extra Ca^{2+} into the SR. The small increase in diastolic $[Ca^{2+}]_i$ amplifies Ca^{2+}-induced-Ca^{2+} release through RyRs, explaining the increased transient amplitudes. This supports the physiological role of background Ca^{2+} entry in increasing Ca^{2+} concentrations. These results replicate prior findings for TRP family members suggested as Ca^{2+} entry channels. For example, we provided evidence for TRPC6 as background Ca^{2+} entry in neonatal rat ventricular

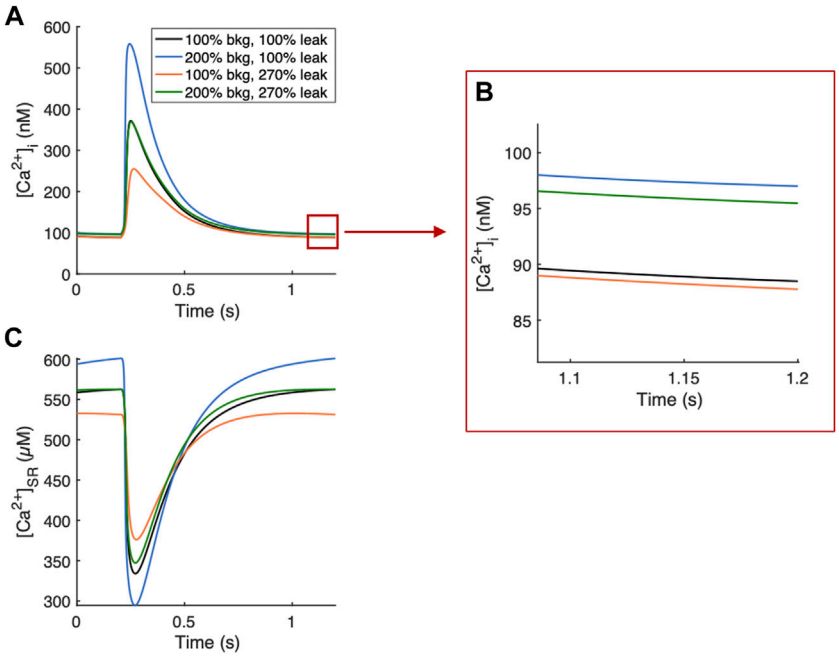

FIGURE 8 | Example Ca^{2+} transients of balanced background Ca^{2+} entry and SR Ca^{2+} leak. **(A)** 200% G_{bkg} and 270% K_{leak} balance their opposing modulations on systolic $[Ca^{2+}]_i$ while increasing diastolic $[Ca^{2+}]_i$ by 7.9%. **(B)** Zoomed-in region demonstrating 7.9% increase in diastolic $[Ca^{2+}]_i$ from default values (black line). **(C)** 200% G_{bkg} and 270% K_{leak} balance opposing effects on SR load.

myocytes (Ahmad et al., 2020). Overexpression of TRPC6 contributes to both elevated $[Ca^{2+}]_i$ and $[Ca^{2+}]_{SR}$. TRPC3 and TRPC6 have also both been implicated in the stress-induced slow increase in $[Ca^{2+}]_i$ and increased $[Ca^{2+}]_i$ transients contributing to the SFR (Seo et al., 2014; Yamaguchi et al., 2017; Yamaguchi et al., 2018). These studies highlight one potential role for Ca^{2+} entry in strained myocytes. Many of the candidates suggested as background Ca^{2+} entry channels are known to be modulated by stretch (Inoue et al., 2009; Reed et al., 2014; Peyronnet et al., 2016), so strained myocytes would exhibit an increase in background Ca^{2+} entry, leading to elevated diastolic levels and larger transients. This mechanism likely contributes to the SFR, increased contractile force following sustained stretch.

SR Ca^{2+} Leak Negatively Modulates Ca^{2+} Concentrations as a Balancing Mechanism

SR Ca^{2+} leak had only a marginal effect on diastolic $[Ca^{2+}]_i$ but reduced $[Ca^{2+}]_{SR}$ and the amplitude of Ca^{2+} transients (**Figure 3**). In general, modulating SR Ca^{2+} leak had the opposite effects of background Ca^{2+} entry, except for the weak effect on diastolic $[Ca^{2+}]_i$. The leaked Ca^{2+} is removed from the cytosol effectively by NCX, which is why it does not affect free cytosolic levels but reduces SR Ca^{2+}. On its own, this complicates the understanding of the physiological role of SR Ca^{2+} leak and the purpose of reduced SR load. When considering the dual-parameter sensitivity analysis, it became however evident that while background Ca^{2+} entry responds to increased needs with increased Ca^{2+}, SR Ca^{2+} leak likely functions as a critical balancing component to regulate SR stores and maintain Ca^{2+} homeostasis. The combined effects of increasing both background Ca^{2+} entry and SR Ca^{2+} leak exhibit a linear relationship, represented by the contour lines of the dual sensitivity plot for systolic $[Ca^{2+}]_i$, $[Ca^{2+}]_i$ amplitude, diastolic and systolic $[Ca^{2+}]_{SR}$ and $[Ca^{2+}]_{SR}$ amplitude (**Figure 7**). If both background and leak currents are modulated along this relationship, measured parameters remain relatively unchanged and only diastolic $[Ca^{2+}]_i$ increases. Examples of balanced background Ca^{2+} entry and SR Ca^{2+} leak in **Figure 8** demonstrate that modulations in G_{bkg} and K_{leak} can be balanced in a way to cancel out the large opposing effects they have on Ca^{2+} transient amplitudes (**Figure 8**). This balancing mechanism of SR Ca^{2+} leak could be critical to prevent Ca^{2+} overload in the cell. Leak in the form of RyR sparks has been demonstrated as SR load regulator to prevent overload, with a steep dependency on $[Ca^{2+}]_{SR}$ (Shannon et al., 2002). However, large Ca^{2+} release events through RyR sparks increase sensitivity for arrhythmia (George, 2008). RyR sparks are most prevalent at high $[Ca^{2+}]_{SR}$, but non-spark RyR leak and non-RyR leak do not appear to exhibit the same steep dependency on $[Ca^{2+}]_{SR}$ and therefore might function differently. Thus, a mechanism of non-RyR leak may be to regulate compartmental Ca^{2+} before the cells become overloaded, and RyR sparks increase as a more extreme measure.

Like channels involved in background Ca^{2+} entry in cardiomyocytes, candidates for SR Ca^{2+} leak also include members of the TRP family and were suggested to be mechano-modulated (Inoue et al., 2009; Reed et al., 2014; Peyronnet et al., 2016). This indicates that the background and leak Ca^{2+} currents could be modulated in conjunction. Non-RyR leak that can be modulated by stretch may provide a more moderate and steady

regulation on a beat-by-beat basis in conjunction with background Ca^{2+} entry modulated by stretch. Recently we demonstrated that TRPC1 constitutes an SR Ca^{2+} leak channel, and its overexpression resulted in decreased SR Ca^{2+} load (Hu et al., 2020). TRPC1 channels are suggested to be modulated by stretch, indicating that the reduction in SR Ca^{2+} load could be a regulatory mechanism to match increased background Ca^{2+} entry through, e.g., TRPC6 channels. We speculate that background Ca^{2+} entry and SR Ca^{2+} leak fulfill a critical homeostatic function in the modulation of Ca^{2+} concentrations throughout the cardiomyocyte in response to strain.

Background and Leak Ca^{2+} Currents May Contribute to Hypertrophy and HF Under Chronic Pressure Overload

Both background Ca^{2+} entry and SR Ca^{2+} leak through TRP channels are likely to be modulated by cardiomyocyte strain (Inoue et al., 2009; Reed et al., 2014; Peyronnet et al., 2016). Under chronic pressure overload conditions, strain-modulation of TRPC channels could increase background Ca^{2+} entry and SR Ca^{2+} leak, and thus dysregulate Ca^{2+}. Cardiac disease is perpetuated by Ca^{2+} dysregulation, and a stray from its homeostatic balance. Some of the suggested ion channels for these Ca^{2+} currents were found to be upregulated in models of cardiac disease, suggesting a role in pathogenesis (Ahmad et al., 2017; Hof et al., 2019). Diastolic $[Ca^{2+}]_i$ is elevated in HF causing diastolic dysfunction (Eisner et al., 2020). Elevated background Ca^{2+} entry could be a contributing factor. Two different models of HF with preserved ejection fraction (HFpEF) display increases in both diastolic and systolic $[Ca^{2+}]_i$ (Curl et al., 2018; Rouhana et al., 2019). A hypothesis is that a major difference in Ca^{2+} handling between HFpEF and HF with reduced ejection fraction (HFrEF) is preserved $[Ca^{2+}]_{SR}$ in HFpEF vs. reduced $[Ca^{2+}]_{SR}$ in HFrEF (Eisner et al., 2020). The decreased SR Ca^{2+} content contributes largely to the decrease in systolic $[Ca^{2+}]_i$ and contractile dysfunction (Bers, 2006). Based on the demonstration of a balancing mechanism between background Ca^{2+} entry and SR Ca^{2+} leak in this study, it is reasonable to speculate a difference between maintenance of this balance in HFpEF vs. a stray from this balanced relationship towards overcompensated leak in HFrEF. In addition to reducing SR Ca^{2+} available for release, causing systolic dysfunction, increased SR Ca^{2+} leak can be problematic, e.g., triggering arrhythmias and being energetically costly due to increased use of ATP to repump Ca^{2+} (Bers, 2014). Understanding the balance of background and leak Ca^{2+} currents in cardiomyocytes and how they affect Ca^{2+} homeostasis and remodeling in disease will be critical to develop effective drug therapies targeting Ca^{2+} channels.

Background and Leak Ca^{2+} Currents are More Effective at Modulating Ca^{2+} at Lower Frequency Pacing

In this study, we observed the well-established frequency dependency of Ca^{2+} transients. Increasing the rate of stimulation increases diastolic $[Ca^{2+}]_i$ in isolated myocytes (Frampton et al., 1991; Antoons et al., 2002; Dibb et al., 2007; Horváth et al., 2017; Sankaranarayanan et al., 2017). Background Ca^{2+} entry and SR Ca^{2+} leak also both exhibit a frequency effect. The parameters we measured are all more sensitive to modulations of the Ca^{2+} currents at slower pacing rates than at faster pacing rates (**Figures 5**, **6**). The sensitivity of each measured $[Ca^{2+}]_i$ and $[Ca^{2+}]_{SR}$ parameter to G_{bkg} and K_{leak} is greatest in amplitude for 1 Hz pacing. An explanation is that at slower pacing rates, the background and leak currents have relatively more time to contribute to the total Ca^{2+} flux per beat vs. the voltage-gated ion channels that open during the action potential and are closed at rest.

Modulation of I_{Cabk} and J_{leak} has Marginal Effects on Action Potentials

Modulating K_{leak} had negligible effects on the action potential for any pacing frequency (**Figure 4**). For the values of K_{leak} tested, we found that the SR Ca^{2+} leak flux does not significantly contribute to sarcolemmal electrophysiology. Modulating G_{bkg} has marginal effects on features of action potentials (**Figure 4**). While G_{bkg} positively correlates with increased resting V_m, an increase to 300% G_{bkg} only resulted in <2% change from basal resting V_m. This minimal change in resting potential is unlikely to be functionally relevant. An increase to 300% G_{bkg} also reduces maximum depolarization by 7% for 1 Hz pacing. The largest effect is an increase in action potential duration (APD90) by around 10% for maximal G_{bkg} modulation. It has also been shown that APD prolongation leads to increased Ca^{2+} (Bouchard et al., 1995), suggesting a positive feedback loop for electrical and Ca^{2+} signaling. Another important note is that APD increase is known to be inotropic, e.g., in rat ventricular myocytes (Bouchard et al., 1995). This indicates another mechanism for the contribution of background Ca^{2+} entry to contractility. Conversely, prolonged APD can induce torsades de pointes tachycardia, leading to life-threatening ventricular fibrillation (Roden and Hoffman, 1985; Ravens and Cerbai, 2008).

Limitations

Mathematical modeling of cellular electrophysiology provides a valuable resource for studying how aspects of cellular physiology interact and affect one another. It provides a means to investigate questions that cannot be easily answered *in vivo*. However, there are also caveats of mathematical modeling that should be considered. It should be noted that the definitions of I_{Cabk} and J_{leak} used in this model are general simplifications and meant to reproduce poorly defined currents. The equations lack specific gating conditions of the currents. The current equations were not parameterized to match experimental data which is only incompletely characterized in human ventricular myocytes. Instead, the current equations are adjusted such that the model reproduces overall physiological action potentials and calcium transients. This is an important consideration, since the magnitudes of these currents could be largely different in living cells. Thus, interpreting the results of this study should focus on the qualitative trends. As the specific ion channels that contribute to Ca^{2+} entry and leak are identified and characterized, future work can aim to refine the current definitions and provide

detailed current models to replace the general simplifications of I_{Cabk} and J_{leak}.

In a similar way, other ion currents in the model are not fully defined. For example, some K^+ channels and isoforms of the Na^+/K^+-ATPase are modulated by localized Ca^{2+} concentrations (Tian and Xie, 2008; Weisbrod, 2020). However, the model does not include any Ca^{2+}-dependent terms in the definitions of these currents. The inclusion of these interactions may alter the effects we see on V_m in this study. Future work could address this limitation.

DATA AVAILABILITY STATEMENT

The original contributions presented in the study are included in the article/**Supplementary Material**, further inquiries can be directed to the corresponding author.

AUTHOR CONTRIBUTIONS

MS and FS designed the study. MS implemented the modeling, analyzed simulation data and drafted the manuscript. All authors critically revised the manuscript and approved the version to be published.

FUNDING

This work was supported by Nora Eccles Treadwell Foundation.

SUPPLEMENTARY MATERIAL

The Supplementary Material for this article can be found online at: https://www.frontiersin.org/articles/10.3389/fphys.2022.916278/full#supplementary-material

REFERENCES

Ahmad, A. A., Streiff, M., Hunter, C., Hu, Q., and Sachse, F. B. (2017). Physiological and Pathophysiological Role of Transient Receptor Potential Canonical Channels in Cardiac Myocytes. *Prog. Biophysics Mol. Biol.* 130, 254–263. doi:10.1016/j.pbiomolbio.2017.06.005

Ahmad, A. A., Streiff, M. E., Hunter, C., and Sachse, F. B. (2020). Modulation of Calcium Transients in Cardiomyocytes by Transient Receptor Potential Canonical 6 Channels. *Front. Physiol.* 11, 44. doi:10.3389/fphys.2020.00044

Ai, X., Curran, J. W., Shannon, T. R., Bers, D. M., and Pogwizd, S. M. (2005). Ca 2+/Calmodulin-Dependent Protein Kinase Modulates Cardiac Ryanodine Receptor Phosphorylation and Sarcoplasmic Reticulum Ca 2+ Leak in Heart Failure. *Circulation Res.* 97, 1314–1322. doi:10.1161/01.res.0000194329.41863.89

Antoons, G., Mubagwa, K., Nevelsteen, I., and Sipido, K. R. (2002). Mechanisms Underlying the Frequency Dependence of Contraction and [Ca 2+] I Transients in Mouse Ventricular Myocytes. *J. Physiology* 543, 889–898. doi:10.1113/jphysiol.2002.025619

Berbey, C., Weiss, N., Legrand, C., and Allard, B. (2009). Transient Receptor Potential Canonical Type 1 (TRPC1) Operates as a Sarcoplasmic Reticulum Calcium Leak Channel in Skeletal Muscle. *J. Biol. Chem.* 284, 36387–36394. doi:10.1074/jbc.m109.073221

Bers, D. M. (2006). Altered Cardiac Myocyte Ca Regulation in Heart Failure. *Physiology* 21, 380–387. doi:10.1152/physiol.00019.2006

Bers, D. M. (2014). Cardiac Sarcoplasmic Reticulum Calcium Leak: Basis and Roles in Cardiac Dysfunction. *Annu. Rev. Physiol.* 76, 107–127. doi:10.1146/annurev-physiol-020911-153308

Bouchard, R. A., Clark, R. B., and Giles, W. R. (1995). Effects of Action Potential Duration on Excitation-Contraction Coupling in Rat Ventricular Myocytes. *Circulation Res.* 76, 790–801. doi:10.1161/01.res.76.5.790

Calaghan, S. C., and White, E. (1999). The Role of Calcium in the Response of Cardiac Muscle to Stretch. *Prog. Biophysics Mol. Biol.* 71, 59–90. doi:10.1016/s0079-6107(98)00037-6

Camacho Londoño, J. E., Tian, Q., Hammer, K., Schröder, L., Camacho Londoño, J., Reil, J. C., et al. (2015). A Background Ca2+entry Pathway Mediated by TRPC1/TRPC4 Is Critical for Development of Pathological Cardiac Remodelling. *Eur. Heart J.* 36, 2257–2266. doi:10.1093/eurheartj/ehv250

Camacho Londoño, J. E., Kuryshev, V., Zorn, M., Saar, K., Tian, Q., Hübner, N., et al. (2021). Transcriptional Signatures Regulated by TRPC1/C4-Mediated Background Ca2+ Entry after Pressure-Overload Induced Cardiac Remodelling. *Prog. Biophys. Mol. Biol.* 159, 86–104. doi:10.1016/j.pbiomolbio.2020.07.006

Chen, M.-S., Xiao, J.-H., Wang, Y., Xu, B.-M., Gao, L., and Wang, J.-L. (2013). Upregulation of TRPC1 Contributes to Contractile Function in Isoproterenol-Induced Hypertrophic Myocardium of Rat. *Cell Physiol. Biochem.* 32, 951–959. doi:10.1159/000354498

Choi, H. S., Trafford, A. W., and Eisner, D. A. (2000). Measurement of Calcium Entry and Exit in Quiescent Rat Ventricular Myocytes. *Pflügers Arch.* 440, 600–608. doi:10.1007/s004240050011

Curl, C. L., Danes, V. R., Bell, J. R., Raaijmakers, A. J. A., Ip, W. T. K., Chandramouli, C., et al. (2018). Cardiomyocyte Functional Etiology in Heart Failure With Preserved Ejection Fraction Is Distinctive-A New Preclinical Model. *J. Am. Heart Assoc.* 7, e007451. doi:10.1161/JAHA.117.007451

Dibb, K. M., Eisner, D. A., and Trafford, A. W. (2007). Regulation of Systolic [Ca2+]iand Cellular Ca2+flux Balance in Rat Ventricular Myocytes by SR Ca2+, L-type Ca2+current and Diastolic [Ca2+]i. *J. Physiol.* 585, 579–592. doi:10.1113/jphysiol.2007.141473

Eisner, D. A., Caldwell, J. L., Trafford, A. W., and Hutchings, D. C. (2020). The Control of Diastolic Calcium in the Heart. *Circ. Res.* 126, 395–412. doi:10.1161/circresaha.119.315891

Frampton, J. E., Orchard, C. H., and Boyett, M. R. (1991). Diastolic, Systolic and Sarcoplasmic Reticulum [Ca2+] during Inotropic Interventions in Isolated Rat Myocytes. *J. Physiol.* 437, 351–375. doi:10.1113/jphysiol.1991.sp018600

George, C. H. (2008). Sarcoplasmic Reticulum Ca2+ Leak in Heart Failure: Mere Observation or Functional Relevance? *Cardiovasc Res.* 77, 302–314. doi:10.1093/cvr/cvm006

Go, L. O., Moschella, M. C., Watras, J., Handa, K. K., Fyfe, B. S., and Marks, A. R. (1995). Differential Regulation of Two Types of Intracellular Calcium Release Channels during End-Stage Heart Failure. *J. Clin. Invest.* 95, 888–894. doi:10.1172/jci117739

Grandi, E., Pasqualini, F. S., and Bers, D. M. (2010). A Novel Computational Model of the Human Ventricular Action Potential and Ca Transient. *J. Mol. Cell. Cardiol.* 48, 112–121. doi:10.1016/j.yjmcc.2009.09.019

Hof, T., Chaigne, S., Récalde, A., Sallé, L., Brette, F., and Guinamard, R. (2019). Transient Receptor Potential Channels in Cardiac Health and Disease. *Nat. Rev. Cardiol.* 16, 344–360. doi:10.1038/s41569-018-0145-2

Horváth, B., Szentandrássy, N., Veress, R., Almássy, J., Magyar, J., Bányász, T., et al. (2017). Frequency-dependent Effects of Omecamtiv Mecarbil on Cell Shortening of Isolated Canine Ventricular Cardiomyocytes. *Naunyn Schmiedeb. Arch. Pharmacol.* 390, 1239–1246.

Hu, Q., Ahmad, A. A., Seidel, T., Hunter, C., Streiff, M., Nikolova, L., et al. (2020). Location and Function of Transient Receptor Potential Canonical Channel 1 in Ventricular Myocytes. *J. Mol. Cell. Cardiol.* 139, 113–123. doi:10.1016/j.yjmcc.2020.01.008

Inoue, R., Jian, Z., and Kawarabayashi, Y. (2009). Mechanosensitive TRP Channels in Cardiovascular Pathophysiology. *Pharmacol. Ther.* 123, 371–385. doi:10.1016/j.pharmthera.2009.05.009

Jones, J. L., Peana, D., Veteto, A. B., Lambert, M. D., Nourian, Z., Karasseva, N. G., et al. (2019). TRPV4 Increases Cardiomyocyte Calcium Cycling and Contractility yet Contributes to Damage in the Aged Heart Following Hypoosmotic Stress. *Cardiovasc Res.* 115, 46–56. doi:10.1093/cvr/cvy156

Kupittayanant, P., Trafford, A. W., Díaz, M. E., and Eisner, D. A. (2006). A Mechanism Distinct from the L-type Ca Current or Na-Ca Exchange Contributes to Ca Entry in Rat Ventricular Myocytes. *Cell Calcium* 39, 417–423. doi:10.1016/j.ceca.2006.01.011

Lemos, F. O., Bultynck, G., and Parys, J. B. (2021). A Comprehensive Overview of the Complex World of the Endo- and Sarcoplasmic Reticulum Ca2+-Leak Channels. *Biochimica Biophysica Acta (BBA) - Mol. Cell Res.* 1868, 119020. doi:10.1016/j.bbamcr.2021.119020

Leybaert, L., Lampe, P. D., Dhein, S., Kwak, B. R., Ferdinandy, P., Beyer, E. C., et al. (2017). Connexins in Cardiovascular and Neurovascular Health and Disease: Pharmacological Implications. *Pharmacol. Rev.* 69, 396–478. doi:10.1124/pr.115.012062

Mijares, A., Altamirano, F., Kolster, J., Adams, J. A., and López, J. R. (2014). Age-dependent Changes in Diastolic Ca2+ and Na+ Concentrations in Dystrophic Cardiomyopathy: Role of Ca2+ Entry and IP3. *Biochem. Biophysical Res. Commun.* 452, 1054–1059. doi:10.1016/j.bbrc.2014.09.045

Peyronnet, R., Nerbonne, J. M., and Kohl, P. (2016). Cardiac Mechano-Gated Ion Channels and Arrhythmias. *Circ. Res.* 118, 311–329. doi:10.1161/circresaha.115.305043

Ravens, U., and Cerbai, E. (2008). Role of Potassium Currents in Cardiac Arrhythmias. *Europace* 10, 1133–1137. doi:10.1093/europace/eun193

Reed, A., Kohl, P., and Peyronnet, R. (2014). Molecular Candidates for Cardiac Stretch-Activated Ion Channels. *Glob. Cardiol. Sci. Pract.* 2014, 9–25. doi:10.5339/gcsp.2014.19

Roden, D. M., and Hoffman, B. F. (1985). Action Potential Prolongation and Induction of Abnormal Automaticity by Low Quinidine Concentrations in Canine Purkinje Fibers. Relationship to Potassium and Cycle Length. *Circ. Res.* 56, 857–867. doi:10.1161/01.res.56.6.857

Rouhana, S., Farah, C., Roy, J., Finan, A., Rodrigues De Araujo, G., Bideaux, P., et al. (2019). Early Calcium Handling Imbalance in Pressure Overload-Induced Heart Failure with Nearly Normal Left Ventricular Ejection Fraction. *Biochimica Biophysica Acta (BBA) - Mol. Basis Dis.* 1865, 230–242. doi:10.1016/j.bbadis.2018.08.005

Rubinstein, J., Lasko, V. M., Koch, S. E., Singh, V. P., Carreira, V., Robbins, N., et al. (2014). Novel Role of Transient Receptor Potential Vanilloid 2 in the Regulation of Cardiac Performance. *Am. J. Physiology-Heart Circulatory Physiology* 306, H574–H584. doi:10.1152/ajpheart.00854.2013

Sankaranarayanan, R., Kistamás, K., Greensmith, D. J., Venetucci, L. A., and Eisner, D. A. (2017). Systolic [Ca2+]i Regulates Diastolic Levels in Rat Ventricular Myocytes. *J. Physiol.* 595, 5545–5555. doi:10.1113/jp274366

Santiago, D. J., Curran, J. W., Bers, D. M., Lederer, W. J., Stern, M. D., Ríos, E., et al. (2010). Ca Sparks Do Not Explain All Ryanodine Receptor-Mediated SR Ca Leak in Mouse Ventricular Myocytes. *Biophysical J.* 98, 2111–2120. doi:10.1016/j.bpj.2010.01.042

Seo, K., Rainer, P. P., Lee, D.-i., Hao, S., Bedja, D., Birnbaumer, L., et al. (2014). Hyperactive Adverse Mechanical Stress Responses in Dystrophic Heart Are Coupled to Transient Receptor Potential Canonical 6 and Blocked by cGMP-Protein Kinase G Modulation. *Circ. Res.* 114, 823–832. doi:10.1161/circresaha.114.302614

Shannon, T. R., Ginsburg, K. S., and Bers, D. M. (2002). Quantitative Assessment of the SR Ca 2+ Leak-Load Relationship. *Circulation Res.* 91, 594–600. doi:10.1161/01.res.0000036914.12686.28

Stout, C. E., Costantin, J. L., Naus, C. C. G., and Charles, A. C. (2002). Intercellular Calcium Signaling in Astrocytes via ATP Release through Connexin Hemichannels. *J. Biol. Chem.* 277, 10482–10488. doi:10.1074/jbc.m109902200

Terracciano, C. M., and Macleod, K. T. (1996). Reloading of Ca(2+)-Depleted Sarcoplasmic Reticulum during Rest in guinea Pig Ventricular Myocytes. *Am. J. Physiology-Heart Circulatory Physiology* 271, H1814–H1822. doi:10.1152/ajpheart.1996.271.5.h1814

Tian, J., and Xie, Z.-j. (2008). The Na-K-ATPase and Calcium-Signaling Microdomains. *Physiology* 23, 205–211. doi:10.1152/physiol.00008.2008

Wang, N., De Bock, M., Antoons, G., Gadicherla, A. K., Bol, M., Decrock, E., et al. (2012). Connexin Mimetic Peptides Inhibit Cx43 Hemichannel Opening Triggered by Voltage and Intracellular Ca2+ Elevation. *Basic Res. Cardiol.* 107, 304. doi:10.1007/s00395-012-0304-2

Ward, M.-L., Williams, I. A., Chu, Y., Cooper, P. J., Ju, Y.-K., and Allen, D. G. (2008). Stretch-activated Channels in the Heart: Contributions to Length-Dependence and to Cardiomyopathy. *Prog. Biophysics Mol. Biol.* 97, 232–249. doi:10.1016/j.pbiomolbio.2008.02.009

Weisbrod, D. (2020). Small and Intermediate Calcium Activated Potassium Channels in the Heart: Role and Strategies in the Treatment of Cardiovascular Diseases. *Front. Physiol.* 11, 590534. doi:10.3389/fphys.2020.590534

Williams, I. A., and Allen, D. G. (2007). Intracellular Calcium Handling in Ventricular Myocytes from Mdx Mice. *Am. J. Physiology-Heart Circulatory Physiology* 292, H846–H855. doi:10.1152/ajpheart.00688.2006

Yamaguchi, Y., Iribe, G., Nishida, M., and Naruse, K. (2017). Role of TRPC3 and TRPC6 Channels in the Myocardial Response to Stretch: Linking Physiology and Pathophysiology. *Prog. Biophysics Mol. Biol.* 130, 264–272. doi:10.1016/j.pbiomolbio.2017.06.010

Yamaguchi, Y., Iribe, G., Kaneko, T., Takahashi, K., Numaga-Tomita, T., Nishida, M., et al. (2018). TRPC3 Participates in Angiotensin II Type 1 Receptor-dependent Stress-Induced Slow Increase in Intracellular Ca2+ Concentration in Mouse Cardiomyocytes. *J. Physiol. Sci.* 68, 153–164. doi:10.1007/s12576-016-0519-3

Zima, A. V., Bovo, E., Bers, D. M., and Blatter, L. A. (2010). Ca2+spark-dependent and -independent Sarcoplasmic Reticulum Ca2+leak in Normal and Failing Rabbit Ventricular Myocytes. *J. Physiol.* 588, 4743–4757. doi:10.1113/jphysiol.2010.197913

Conflict of Interest: The authors declare that the research was conducted in the absence of any commercial or financial relationships that could be construed as a potential conflict of interest.

Publisher's Note: All claims expressed in this article are solely those of the authors and do not necessarily represent those of their affiliated organizations, or those of the publisher, the editors and the reviewers. Any product that may be evaluated in this article, or claim that may be made by its manufacturer, is not guaranteed or endorsed by the publisher.